nature geoscience

LETTERS

PUBLISHED ONLINE: 23 SEPTEMBER 2012 | DOI: 10.1038/NGEO1586

A stratospheric connection to Atlantic climate variability

Thomas Reichler[1]*, Junsu Kim[1], Elisa Manzini[2] and Jürgen Kröger[2]

The stratosphere is connected to tropospheric weather and climate. In particular, extreme stratospheric circulation events are known to exert a dynamical feedback on the troposphere[1]. However, it is unclear whether the state of the stratosphere also affects the ocean and its circulation. A co-variability of decadal stratospheric flow variations and conditions in the North Atlantic Ocean has been suggested, but such findings are based on short simulations with only one climate model[2]. Here we assess ocean reanalysis data and find that, over the previous 30 years, the stratosphere and the Atlantic thermohaline circulation experienced low-frequency variations that were similar to each other. Using climate models, we demonstrate that this similarity is consistent with the hypothesis that variations in the sequence of stratospheric circulation anomalies, combined with the persistence of individual anomalies, significantly affect the North Atlantic Ocean. Our analyses identify a previously unknown source for decadal climate variability and suggest that simulations of deep layers of the atmosphere and the ocean are needed for realistic predictions of climate.

The ocean has a large thermal inertia and is dominated by variability on timescales of years to decades. Traditionally, atmospheric influences on the ocean are understood from the stochastic climate model paradigm, in which the troposphere is thought to provide a white-noise forcing that is integrated by the ocean to yield a low-frequency response[3]. In this study we propose another relevant influence, which is related to the stratosphere. The stratosphere is characterized by persistent flow dynamics[4] and considerable multi-decadal energy[5–7]. Variations in the strength of the wintertime northern hemispheric stratospheric vortex, so called 'polar vortex events', are known to last for many weeks, as does their impact on the troposphere[8]. An example is stratospheric sudden warmings (SSWs), prolonged time periods with an unusually weak and warm polar vortex. SSWs occur on average every second year, but observations over the past 30 years reveal an intriguing quasi-decadal rhythm in the year-to-year occurrence of such events: during the 1990s, the Arctic winter stratosphere was characterized by an almost complete absence of SSWs, but during the 1980s and also during the 2000s the stratosphere experienced a record number of such events (Fig. 1a).

A connection between the stratosphere and the ocean can be established by the North Atlantic Oscillation (NAO), a large-scale pattern of near-surface circulation anomalies over the North Atlantic. Polar vortex events modulate the NAO polarity, with a strong vortex leading to a positive and a weak vortex to a negative NAO (ref. 8). NAO variations in turn are linked to circulation variability in the North Atlantic. The NAO induces anomalous

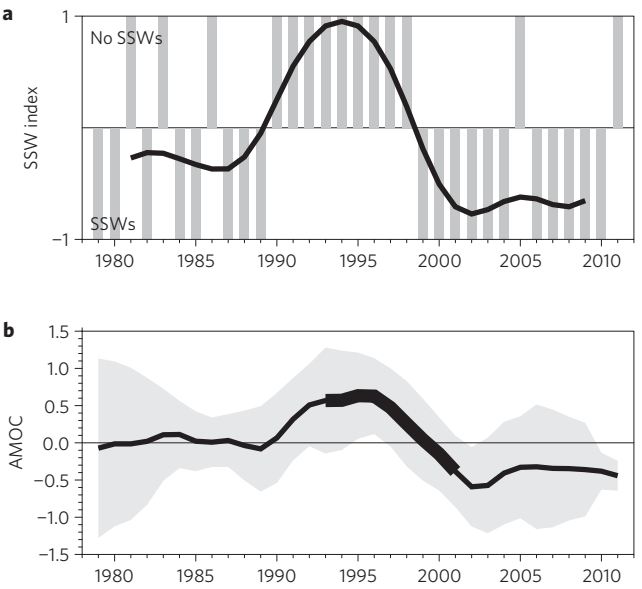

Figure 1 | Observed stratospheric flow variations and their relationship to AMOC. a, Annual time series of the SSW index; grey bars mark years with (−1) and without (1) major SSWs; the black line is a smoothed version of this. **b**, Multi-reanalysis estimate of annual mean AMOC variations at 45° N; thick black line denotes the common period for all 12 reanalyses and grey shading is the $\pm 1\sigma$ uncertainty interval.

fluxes of heat, momentum, and freshwater at the air–sea interface, driving or perhaps enhancing intrinsic variability in the North Atlantic gyre system[9] and the Atlantic Meridional Overturning Circulation[10,11] (AMOC). Thus, variations in the strength of the polar vortex and their projection on the NAO might influence the North Atlantic circulation. This is supported by a reconstruction of past AMOC variations using twelve different ocean reanalyses, revealing a similarity between variations in the AMOC (Fig. 1b) and the frequency of SSWs (Fig. 1a).

The observational record is too short for a rigorous analysis of multi-decadal variability. Therefore, we examine the climate model GFDL-CM2.1, which was integrated for 4,000 years with constant forcings, approximately representative for pre-industrial conditions[12]. A connection between stratosphere and ocean depends on the downward coupling into the troposphere. We examine this coupling by comparing the simulation against atmospheric reanalysis (hereafter simply observations). Focusing on periods where the polar vortex is unusually strong, we define

[1]Department of Atmospheric Sciences, University of Utah, Salt Lake City, Utah 84103, USA, [2]Max Planck Institute for Meteorology, Hamburg 20146, Germany. *e-mail: thomas.reichler@utah.edu.

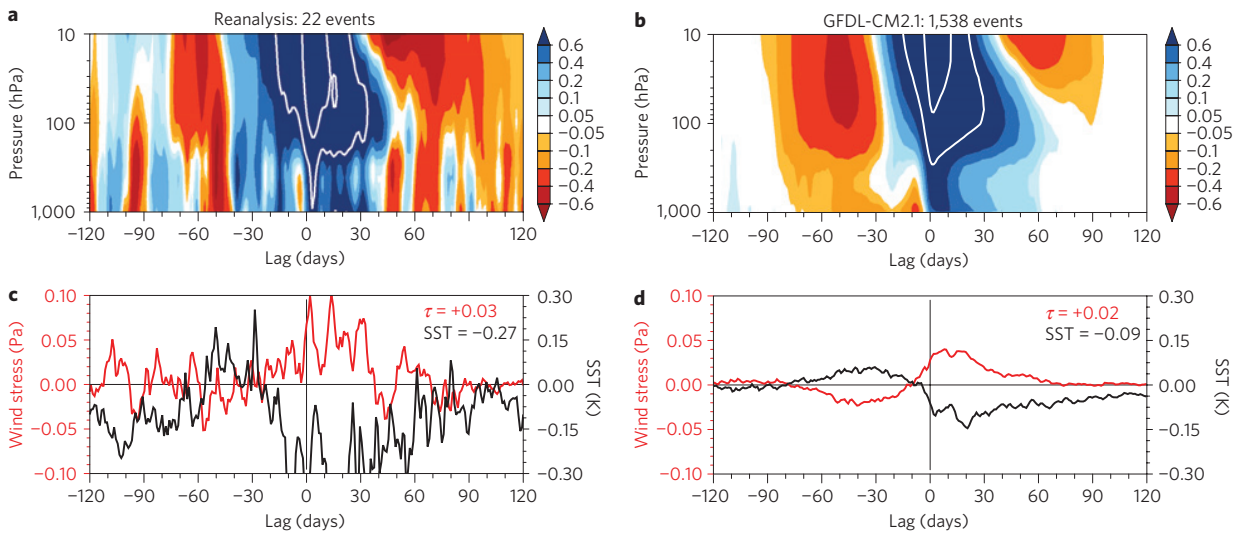

Figure 2 | Strong polar vortex composites and their surface impact. a,**b**, Time–height development of the NAM index; white contours indicate NAM values of 1 and 2. Horizontal time axis indicates the lead or lag (in days) with respect to the date of the events. The events are determined by the dates on which the NAM at 10 hPa exceeds +2.5. **c**,**d**, Associated (red) zonal wind stress and (black) SST anomalies over the North Atlantic study region; numbers at the upper right are averages over days 0–60.

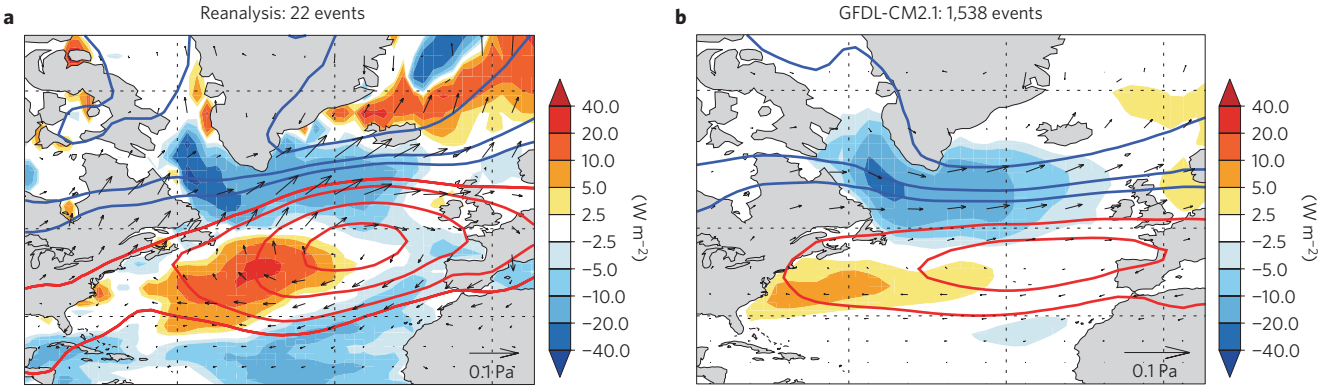

Figure 3 | Spatial pattern of surface impact from the stratosphere. Shown are composite anomalies averaged from day 0 to 60 following the strong vortex events of Fig. 2. Sea-level pressure anomalies are contoured at ±0.5, ±1, ±2, ±3, ±4 hPa; red and blue lines indicate positive and negative values, respectively. Shading shows the sum of latent and sensible heat flux anomalies (in W m^{-2}), with positive and negative anomalies indicating oceanic heat gain and loss, respectively. Vectors represent the magnitude and direction of surface wind stress anomalies.

events during which the Northern Annular Mode index (NAM) at 10 hPa crosses a threshold of 2.5. Our outcomes are not very sensitive to the exact threshold, but our choice limits the number of events and captures sufficiently strong events. In the observations, we find 22 events, which is an average of four per decade. At 3.8 per decade, the model produces similar statistics. We form composites of observed and simulated events in terms of anomalies in the NAM at pressure levels between 1,000 and 10 hPa and for various lags. The model captures well the structure of downward propagating stratospheric NAM anomalies seen in the observations (Fig. 2a,b). However, the NAM is normalized and thus not an absolute measure of circulation anomaly. This is important, because the model does not have a well-resolved stratosphere, and, compared to the observations, it underestimates the day-to-day variability of zonal mean zonal winds in the stratosphere by about 40%. A more objective response measure is the zonal wind stress (τ) over our North Atlantic study region (15° W–60° W, 45° N–65° N). For the selected events, the simulated τ anomalies are considerably smaller than in the observations (Fig. 2c,d), which is probably a consequence of the inadequate treatment of the model's stratosphere. However, it is reassuring that the model reproduces the observed sign and temporal structure of τ.

The surface impacts of the events examined in Fig. 2 include a north–south dipole in sea level pressure, which is a positive phase of the NAO (Fig. 3). The nodal point of this dipole is located to the south of Greenland. There, the changes in wind stress amplify the climatological mean westerlies and heat fluxes that extract thermal energy from the ocean. The model produces a heat flux pattern (Fig. 3 shading) that is very similar to the observations, but the sea surface temperature (SST) cooling over the study region is three times smaller (Fig. 2c,d). This muted SST response is related to the weak wind stress forcing, but also to the model's heat distribution in a 10 m-thick top ocean layer. The cooling to the south of Greenland is dynamically relevant because it is colocated with sites of significant deepwater formation in the Labrador and Irminger Seas and with the model's subpolar gyre (SPG; Supplementary Fig. S2).

We now study the ocean response in GFDL-CM2.1 to the stratospherically induced cooling. Because low-frequency forcing should be most effective in driving the ocean[3], we composite on a low-pass filtered stratospheric NAM (see Methods) using a

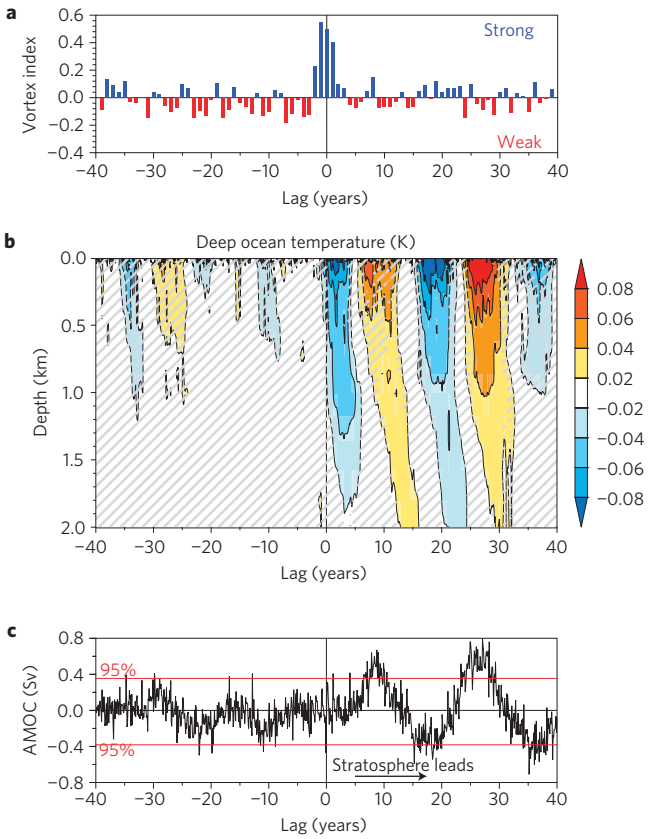

Figure 4 | Impact of persistent stratospheric flow variations. Shown are GFDL-CM2.1 derived composites of periods during which the polar vortex was either persistently strong (75 events) or persistently weak (70 events, multiplied by −1). **a**, Composite time series of the vortex index, measuring the likelihood that a vortex event happens during a given year. The index represents a composite and therefore varies smoothly between +1 and −1. **b**, Corresponding monthly time–depth development of ocean temperature anomalies (K) over the study region (15° W–60° W, 45° N–65° N); hatching shows insignificant (95%) results. **c**, Corresponding monthly anomalies in AMOC strength (Sv).

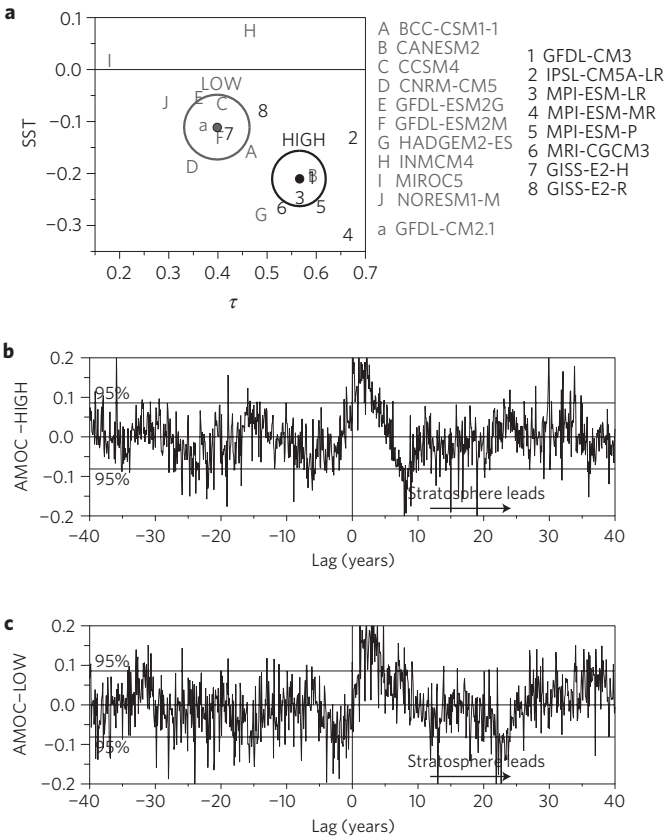

Figure 5 | CMIP5 composites on stratospheric NAM. a, Standardized τ and SST anomalies over study region for individual models and mean of all low-top and all high-top models; the anomalies are averages over months 1–2 (τ) and 1–3 (SST) following the NAM events. Thresholds of +2.5 and −3 in monthly NAM define the events. Circles are 95% uncertainty intervals (see Methods). **b**,**c**, Standardized AMOC anomalies from the high-top (low-top) models composited on persistent NAM events; the events are defined as in Fig. 4 and contain 127 (143) strong and 133 (144) weak events for LOW (HIGH).

threshold of ±1. From the 4,000 years, we identify 75 strong and 70 weak events. Results from weak events are multiplied by −1 and combined with the strong events to form a single composite. The vortex index (Fig. 4a), which reflects the likelihood for a vortex event to occur, shows the outcome of the compositing in terms of stratospheric circulation anomalies: the compositing favours strong polar vortex events that happen for several consecutive years centred on year zero. This situation is comparable to the one seen in the observations over the past 30 years (Fig. 1a).

Over our study region, the vortex events induce a ∼0.1°K cooling at the ocean surface (Fig. 4b). Over the course of a few years, this signal penetrates into the deep ocean. The speed and depth of the penetration suggest that deep convection, which prevails over this region, is responsible. The cooling is followed by regular oscillations, which have a similar periodicity as the model's AMOC (Supplementary Fig. S1). This suggests that the oscillations are connected to the AMOC, which is confirmed when compositing the AMOC on the stratospheric events (Fig. 4c). Following the central date, the AMOC undergoes regular fluctuations that are coherent with the ocean temperatures.

The standard deviation of the low-pass filtered AMOC fluctuations following the central date amounts to ∼0.23 Sv (Fig. 4c). However, for certain strong events this value exceeds ∼0.5 Sv (Supplementary Fig. S3), which can be compared to the ∼1.3 Sv of the model's total AMOC standard deviation. In other words, forcing from the stratosphere contributes to a large portion of total AMOC variability. The vigorous intrinsic tendency of the model's AMOC to oscillate suggests that the stratosphere acts as trigger for such oscillations and that forcing at the resonant frequency is most effective in driving it. This is supported by analysis presented in Supplementary Fig. S3.

We generalize our results by investigating further simulations taken from the preindustrial control experiment of the Fifth Coupled Model Intercomparison Project (CMIP5). For each CMIP5 model, we examine the surface anomalies that develop over the study region in response to vortex events (Fig. 5a). As before, strong events are associated with increased τ and colder SSTs, but there is a large inter-model spread. We divide the models into two classes: high-top models with a well-resolved stratosphere, and low-top models with a relatively simple stratosphere. The surface response of the combined (black) high-top models is significantly stronger than that of the (grey) low-top models, confirming our previous assumption about the role of stratospheric representation. Using criteria identical to that in Fig. 4, we composite the AMOC time series from all high-top (Fig. 5b) and all low-top (Fig. 5c) models on low-frequency vortex events. As in GFDL-CM2.1, the AMOC of both multi-model ensembles starts to oscillate after the vortex events. However, whereas the oscillations persist for decades in GFDL-CM2.1, they vanish after several years in the CMIP5

ensembles. This is due to the widely differing spectral characteristics of the AMOC in the models, leading the composite outcome to de-correlate relatively fast. The magnitude of the AMOC anomalies after the events reaches ∼20% of the climatological standard deviation. It is about the same for the two model classes, despite the differences in forcing strength at the surface. This similarity might be related to model differences that go beyond our simple high-top/low-top classification and the complicated response of the AMOC, which involves nonlinear dynamics.

Our analysis suggests a significant stratospheric impact on the ocean. Recurring stratospheric vortex events create long-lived perturbations at the ocean surface, which penetrate into the deeper ocean and trigger multi-decadal variability in its circulation. This leads to the remarkable fact that signals that emanate from the stratosphere cross the entire atmosphere–ocean system. The propagation into the deeper ocean can be explained from the well-known impact of the NAO on the SPG and AMOC (refs 13,14). The oscillatory behaviour of the ocean following stratospheric events is probably related to a delayed negative feedback of the AMOC on itself[11,14,15]. A number of factors promote the stratosphere–ocean connection: the persistence of individual stratospheric events; a stratospheric rhythm that matches the resonant frequency of the AMOC; the dynamical coupling from the stratosphere to the troposphere; the collocation between the NAO nodal point and regions of downwelling; and the intrinsic instability of the AMOC.

We do not advocate the stratosphere as the sole or primary source of AMOC variability. However, the stratosphere seems to contain a significant amount of low-frequency energy capable of modulating the AMOC. The source of this energy may be related to coupling with other subcomponents of climate[16–18] or variations in external forcings[19,20]. However, in our simulations external forcings are held constant in time, and our analysis (Fig. 4 and Supplementary Figs S4 and S5) leads to the conclusion that at low frequencies the stratosphere drives the AMOC. It seems most likely to us that the stratospheric multi-decadal energy is related to stochastic forcing from the troposphere[21,22], which may involve variations in the dynamical wave forcing[7], or in the frequency of blockings[23] and their influence on SSWs (ref. 24).

Our results have implications for the prediction of decadal climate, an subject that has gained increasing attention recently[25–27]. As it is impossible to accurately predict variations in the strength of the polar vortex beyond several days, it is likely that the new mechanism acts to limit the skill of decadal predictions. However, representing the coupling between stratosphere, troposphere, and ocean in modelling systems should refine estimates of decadal climate predictability and improve the skill of short-term climate predictions after strong stratospheric events. Our results add to an increasing body of evidence that the stratosphere forms an important component of climate and that this component should be represented well in models.

Methods

Data

Observations. NCEP/NCAR reanalysis (1958–2011) are used as observations of geopotential height, surface fluxes and SSTs.

GFDL-CM2.1. The main model of this study is the Geophysical Fluid Dynamics Laboratory climate model GFDL-CM2.1. It has a horizontal resolution of 2° latitude by 2.5° longitude, and 24 vertical levels concentrated in the troposphere, leading to a relatively poorly resolved stratosphere. The model produces realistic simulations of tropospheric climate[28] and self-sustained AMOC oscillations with a central period of ∼20 years (Supplementary Fig. S1). Such oscillations may be connected to the Atlantic Multi-decadal Oscillation[29] (AMO), a pattern of North Atlantic SST variations with a period of 60–80 years[30]. The fact that the period of the observed AMO is longer than the period of the simulated AMOC is not surprising given the many simplifying physics in climate models and the uncertainty in observing the AMO.

CMIP5. CMIP5 data are based on monthly means from the preindustrial control experiment. We consider models that provide at least 500 years of data and the quantities needed for our analysis. This leads to 18 models with a total of 12,944 years of simulation data (Fig. 5a and Supplementary Table S2). In Fig. 5b,c we perform analysis on the concatenated NAM and AMOC time series from models belonging to either the high-top or the low-top group; time series from each model are standardized before concatenation.

Statistics

Statistical analysis. In all our analysis we take the same non-parametric approach to establish statistical significance at the two-sided 95% level. In this approach, we randomly sub-sample elements from the entire population and take averages. The number of elements selected equals the number included in the quantity to be tested. We repeat this procedure 10,000 times, leading to a distribution of outcomes that is the result of pure chance. The upper and lower 2.5 percentiles of this distribution are our empirically determined confidence limits.

Event selection. The events selected for the composites shown in Figs 4 and 5b,c are based on the dates on which the smoothed annual November–March means of the NAM at 10 hPa (Gaussian filter, $\sigma \sim 2$ years) exceed a value of ± 1; selected events are separated by at least 30 years.

Detrending. To account for long-term trends we first remove from all quantities a low-pass filtered (101-year running means) version of the data. Daily atmospheric quantities are filtered by removing a slowly varying trend climatology, following a procedure that accounts for seasonality of trends[31], except that a running mean filter of 101 years is applied.

Climate indices

SSWs. SSWs are defined when the daily zonal mean zonal wind at 10 hPa becomes easterly. Only the first SSW in a given winter is chosen; final warmings are excluded.

SSW index. The binary SSW index is defined by assigning years with (without) a SSW a value of -1 ($+1$).

Vortex index. The model derived 'vortex index' is similar to the 'SSW index'; both measure whether a polar vortex event occurs. Introducing the vortex index is necessary because most low-top models have positive stratospheric wind biases, causing wind reversals and SSWs to become rare. The vortex index is based on the daily normalized NAM at 10 hPa and a threshold of $+2$ (-3) to identify strong (weak) vortex years. The index is assigned a value of $+1$ (-1) if a strong (weak) vortex is detected; other years (neutral) are assigned a value of zero.

NAM. The NAM is based on empirical orthogonal function (EOF) analysis performed individually at each level using daily zonal mean geopotential heights poleward of 20° N; the NAM is the standardized EOF time series at any level.

NAO. The NAO is the leading EOF time series of daily sea level pressure over 20° N–80° N and 90° W–40° E.

AMOC. The AMOC is the maximum of the North Atlantic meridional overturning streamfunction at 45° N. For some models, the streamfunction is available as a pre-calculated CMIP5 quantity. For other models and for the reanalyses, the streamfunction is derived by vertically integrating the meridional sea water velocity. The reanalysis derived AMOC (1979–2010) stems from the mean over 12 products (Supplementary Table S1). Before taking the multi-reanalysis mean, time series from each reanalysis are normalized, annually averaged, and smoothed (Gaussian filter, $\sigma \sim 1.3$ years). All 12 reanalysis are only available for the 1993–2001 period. Outside this period, fewer reanalyses exist, creating spurious discontinuities at the interface between the full and the reduced set. We adjust for this by removing from the reduced set the difference between the full and reduced set at the interface.

AMO. The AMO is the monthly mean SST average over 0° N–60° N and 75° W–7.5° W (ref. 19).

Received 30 March 2012; accepted 17 August 2012; published online 23 September 2012

References

1. Baldwin, M. P., Thompson, D. W. J., Shuckburgh, E. F., Norton, W. A. & Gillett, N. P. Weather from the stratosphere? *Science* **301,** 317–319 (2003).
2. Manzini, E., Cagnazzo, C., Fogli, P. G., Bellucci, A. & Müller, W. A. Stratosphere–troposphere coupling at inter-decadal time scales: Implications for the North Atlantic Ocean. *Geophys. Res. Lett.* **39,** L05801 (2012).
3. Hasselmann, K. Stochastic climate models Part I. Theory. *Tellus* **28,** 473–485 (1976).
4. Baldwin, M. P. *et al.* Stratospheric memory and extended-range weather forecasts. *Science* **301,** 636–640 (2003).
5. Cohen, J., Barlow, M. & Saito, K. Decadal fluctuations in planetary wave forcing modulate global warming in late boreal winter. *J. Clim.* **22,** 4418–4426 (2009).

6. Gillett, N. P. *et al.* How linear is the Arctic Oscillation response to greenhouse gases? *J. Geophys. Res.* **107,** 4022 (2002).
7. Butchart, N., Austin, J., Knight, J. R., Scaife, A. A. & Gallani, M. L. The response of the stratospheric climate to projected changes in the concentrations of well-mixed greenhouse gases from 1992 to 2051. *J. Clim.* **13,** 2142–2159 (2000).
8. Baldwin, M. P. & Dunkerton, T. J. Stratospheric harbingers of anomalous weather regimes. *Science* **294,** 581–584 (2001).
9. Hakkinen, S. & Rhines, P. B. Decline of subpolar North Atlantic circulation during the 1990s. *Science* **304,** 555–559 (2004).
10. Delworth, T. L. & Greatbatch, R. J. Multidecadal thermohaline circulation variability driven by atmospheric surface flux forcing. *J. Clim.* **13,** 1481–1495 (2000).
11. Eden, C. & Jung, T. North Atlantic interdecadal variability: Oceanic response to the North Atlantic Oscillation (1865–1997). *J. Clim.* **14,** 676–691 (2001).
12. Wittenberg, A. T. Are historical records sufficient to constrain ENSO simulations? *Geophys. Res. Lett.* **36,** L12702 (2009).
13. Häkkinen, S. Variability of the simulated meridional heat transport in the North Atlantic for the period 1951–1993. *J. Geophys. Res.* **104,** 10991–11007 (1999).
14. Lohmann, K., Drange, H. & Bentsen, M. A possible mechanism for the strong weakening of the North Atlantic subpolar gyre in the mid-1990s. *Geophys. Res. Lett.* **36,** L15602 (2009).
15. Delworth, T., Manabe, S. & Stouffer, R. J. Interdecadal variations of the thermohaline circulation in a coupled ocean–atmosphere model. *J. Clim.* **6,** 1993–2011 (1993).
16. Msadek, R., Frankignoul, C. & Li, L. Mechanisms of the atmospheric response to North Atlantic multidecadal variability: A model study. *Clim. Dynam.* **36,** 1255–1276 (2011).
17. Mosedale, T. J., Stephenson, D. B., Collins, M. & Mills, T. C. Granger causality of coupled climate processes: Ocean feedback on the North Atlantic oscillation. *J. Clim.* **19,** 1182–1194 (2006).
18. Cohen, J., Barlow, M., Kushner, P. J. & Saito, K. Stratosphere–troposphere coupling and links with Eurasian land surface variability. *J. Clim.* **20,** 5335–5343 (2007).
19. Ottera, O. H., Bentsen, M., Drange, H. & Suo, L. External forcing as a metronome for Atlantic multidecadal variability. *Nature Geosci.* **3,** 688–694 (2010).
20. Ineson, S. *et al.* Solar forcing of winter climate variability in the Northern Hemisphere. *Nature Geosci.* **4,** 753–757 (2011).
21. Scaife, A. A., Knight, J. R., Vallis, G. K. & Folland, C. K. A stratospheric influence on the winter NAO and North Atlantic surface climate. *Geophys. Res. Lett.* **32,** L18715 (2005).
22. Plumb, R. A. & Semeniuk, K. Downward migration of extratropical zonal wind anomalies. *J. Geophys. Res.* **108,** 4223 (2003).
23. Hakkinen, S., Rhines, P. B. & Worthen, D. L. Atmospheric blocking and Atlantic multidecadal ocean variability. *Science* **334,** 655–659 (2011).
24. Martius, O., Polvani, L. M. & Davies, H. C. Blocking precursors to stratospheric sudden warming events. *Geophys. Res. Lett.* **36,** L14806 (2009).
25. Keenlyside, N. S., Latif, M., Jungclaus, J., Kornblueh, L. & Roeckner, E. Advancing decadal-scale climate prediction in the North Atlantic sector. *Nature* **453,** 84–88 (2008).
26. Smith, D. M. *et al.* Skilful multi-year predictions of Atlantic hurricane frequency. *Nature Geosci.* **3,** 846–849 (2010).
27. Mehta, V. *et al.* Decadal climate predictability and prediction: Where are we? *Bull. Am. Meteorol. Soc.* **92,** 637–640 (2011).
28. Reichler, T. & Kim, J. How well do coupled models simulate today's climate? *Bull. Am. Meteorol. Soc.* **89,** 303–311 (2008).
29. Delworth, T. L. & Mann, M. E. Observed and simulated multidecadal variability in the Northern Hemisphere. *Clim. Dynam.* **16,** 661–676 (2000).
30. Schlesinger, M. E. & Ramankutty, N. An oscillation in the global climate system of period 65–70 years. *Nature* **367,** 723–726 (1994).
31. Gerber, E. P. *et al.* Stratosphere–troposphere coupling and annular mode variability in chemistry-climate models. *J. Geophys. Res.* **115,** D00M06 (2010).

Acknowledgements

We thank T. Delworth, P. Staten and C. Strong for their comments on an earlier version of this work. We thank the Geophysical Fluid Dynamics Laboratory for making the CM2.1 simulation data available to us. We acknowledge the World Climate Research Programm's Working Group on Coupled Modelling, which is responsible for CMIP, and we thank the climate modelling groups for producing and making available their model output. For CMIP, the US Department of Energy's Program for Climate Model Diagnosis and Intercomparison provides coordinating support and led development of software infrastructure in partnership with the Global Organization for Earth System Science Portals. This research used resources of the National Energy Research Scientific Computing Center, which is supported by the Office of Science of the US Department of Energy under Contract No. DE-AC02-05CH11231. T.R. and J.K. were supported by the University of Utah. E.M. and J.K. are grateful for partial funding by the European Commission's 7th Framework Programme, under GA 226520, COMBINE project. Provision of computer infrastructure by the Center for High Performance Computing at the University of Utah is gratefully acknowledged.

Author contributions

T.R. designed the research and wrote the manuscript. J. Kim carried out the analysis. All authors contributed to the interpretations of the results and the discussion of the manuscript.

Additional information

Supplementary information is available in the online version of the paper. Reprints and permissions information is available online at www.nature.com/reprints. Correspondence and requests for materials should be addressed to T.R.

Competing financial interests

The authors declare no competing financial interests.